Extension-induced dispersion of multi-walled carbon nanotube in non-Newtonian fluid

Joung Sook Hong and Chongyoup Kim[a)]

Department of Chemical and Biological Engineering, Korea University, Anam-dong, Sungbuk-ku, Seoul 136-713, Korea

(Received 25 September 2006; final revision received 1 June 2007)

Synopsis

In this study, we devised an extension-induced mixer to disperse carbon nanotube (CNT) clumps into individual tubes by imposing extensional stress continuously and periodically. The rheological behavior of the CNT-dispersed suspension was investigated to examine whether the hydrodynamic dragging induces the dispersion of individual CNT from strongly entangled CNT by van der Waals force between adjacent tubes. When CNT clumps were subjected to a continuous extensional flow for a prolonged time, the optical microscopic and cryo-transmission electron microscopy studies showed that the CNT agglomerates were effectively dispersed and some of the individual nanotubes were disentangled from the CNT clump. Shear viscosity of the dispersion increased when the CNT-Boger fluid suspension was subjected to the continuous and periodic extensional flow for a prolonged time, indicating the dispersion of the individual tubes by the extensional flow. Under shear flows, however, aggregated CNT clumps formed larger, weakly bound agglomerates with diameters up to millimeters. The newly suggested mixing technique can be used effectively for mixing two different kinds of polymers with a large difference in viscosity. © *2007 The Society of Rheology.* [DOI: 10.1122/1.2751384]

I. INTRODUCTION

The impressive mechanical, electrical and thermal properties of carbon nanotube have attracted great interest since the discovery by Iijima (1991). The strength and flexibility of carbon nanotubes make them of potential use in controlling nanoscale structures of polymer composite, biomedical and electrical applications to pursue reinforcing, selective bonding or alignment. Almost all the carbon nanotubes (CNTs) are not straight and remain as entangled aggregates due to van der Waals attraction [Harris (1999)]. However, the unique properties and potentials of nanotube are realized only when CNTs are well dispersed in the medium and the microstructure of the mixture can be controlled. Especially, only if there is no difficulty in dispersing, the various properties of CNT can be successfully used for most applications. For example, in the application of CNT to the electron guns of field emission displays, CNTs have to be disentangled and aligned to eject enough number of electrons under a given electric field. Therefore, most recent research on carbon nanotube has been carried out on dispersion [Bandyopadhyaya *et al.* (2002); Bar-Chaput and Carrot (2006); Huang *et al.* (2006)] as well as production and application [Dwyer *et al.* (2002)].

[a)]Author to whom correspondence should be addressed; electronic mail: cykim@grtrkr.korea.ac.kr

To disperse the entangled carbon nanotubes in fluid, usually the ionic force between nanotube and solvent is used to overcome the van der Waals force between entangled nanotubes [Zhou *et al.* (2003); Matarredona *et al.* (2003); Li *et al.* (2003); Sano *et al.* (2001); Xu *et al.* (2005)]. However, this method requires the usage of acid solvents and it brings out damage in CNT surfaces as well as some environmental problems due to the usage of toxic chemicals. Therefore, it is necessary to study more on the dispersion of CNT from many diverse viewpoints and to develop new, alternative methods of dispersion. Another issue in the dispersion of CNTs is that the widely used microscopy cannot be an adequate method and therefore an alternative method is needed to evaluate the degree of dispersion. This is because the optical microscopy cannot resolve the small length scales of CNT and the electron microscopy is basically a surface technique while mixing is a bulk phenomenon [Huang *et al.* (2006)]. To overcome this problem, Huang *et al.* monitored the rheological properties of dispersion as mixing continued and found that a critical mixing time, t^*, which was a function of nanotube concentration and the shear stress in the mixing device, had to be exceeded to achieve satisfactory dispersion of aggregates in the case of Newtonian fluid. They also used the rheological approach to determine the effect of aging and reaggregation.

In CNT suspension, there is fluid mechanical friction (dragging) between the suspending fluid and CNT clumps depending on flow field. If a sufficiently strong external hydrodynamic force is continuously imposed on CNT suspension, the hydrodynamic force makes individual tubes crawled out from the CNT entangled clumps. Especially under tensional fields, the friction is maximized and the possibility of collision between CNT clumps is reduced. In this study, we devised a set of equipment that can realize the extensional flow to induce the hydrodynamic friction (dragging) continuously between CNT and the suspending fluid. The extensional flow of a fluid band is established mechanically from the intercross of two parallel bars that hold the band against the other bar fixed at the center of two parallel bars, which makes it possible to stretch a fluid without dripping (breakup) over several days. For the stretching of a fluid band, we need to use viscoelastic fluids and we cannot use Newtonian fluids because they drip in the gravitational field without being stretched, especially at the initial stage of mixing. Therefore, the elasticity of fluid is essential. In this research, Boger fluids are chosen as the suspending fluid because Boger fluid is elastic and it is easy to control its viscosity and elasticity. It has been found that the extensional flow is a very effective method of reducing the size of CNT clumps and the disentanglement of individual tubes from the clump.

II. EXPERIMENT

A. Materials

Carbon nanotubes (CNTs) used in this study are multi-walled, commercial grade nanotubes (purity $>90\%$, manufacturer's specification) supplied from Iljin Nanotech, Korea. We dispersed CNTs in a suspending medium as received from the manufacturer. It is known from the manufacturer that the CNT is prepared by a chemical vapor deposition method by the reaction of a carbon-containing gas such as acetylene, ethylene, ethanol, etc., with a metal catalyst at above 600 °C. The diameter and the length of the tube are in the range of 10–20 nm and 10–50 μm, respectively. As shown in Fig. 1, CNTs are entangled to form clumps. Each clump has a nearly spherical shape with the diameter of a broad distribution from 10 to several hundreds micron size. Figure 1(c) shows the four vials containing CNT dispersions of 0.05 wt% CNT after three months. CNTs were dispersed in water or organic solvent with or without a dispersant with a varying charge

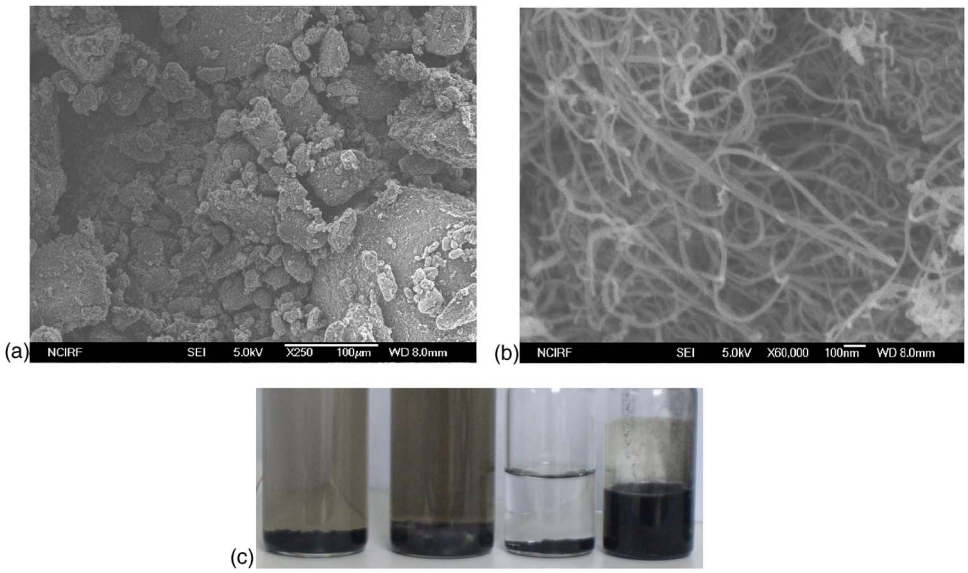

FIG. 1. SEM pictures of carbon nanotube clumps ((a) 250x, (b) 60,000x). (c) is the sedimentation test of carbon nanotube in vials with four different solutions: from left, 5 wt% sodiumdodecyl sulfate, 5 wt% dodecyltrimethyl-ammoniumbromide, 2-chloropropane, and PIB/PB.

level to test the ability of additive in dispersing CNT: (a) 5 wt% sodiumdodecyl sulfate (negatively charged); (b) 5 wt% dodecyltrimethyl-ammoniumbromide (positively charged); (c) 2-chloropropane (not charged); (d) polyisobutylene/polybutane (PIB/PB) solution (not charged). In solutions a, b and c, CNTs were mostly agglomerated at the bottom of the vial. In solution d, the uniformly dispersed state of CNT was preserved except for a small portion of coagulates at the bottom. Therefore, as the suspending medium, PB/PIB solutions were chosen in this study. PIB/PB solutions are known as a Boger fluid that is a dilute solution of an ultra high molecular weight polymer in a very viscous Newtonian solvent [Magda and Larson (1998)]. The Boger fluids used in this study are composed of polyisobutylene (PIB: M_n=3.1 M, Sigma-Aldrich Chem. Co.) in polybutene (PB M_n=920, Sigma-Aldrich Chem. Co.). PB has a density of 890 kg/m^3 and a viscosity of 21 Pa s at 25 °C. The content of PIB in PB is varied from 0.1 to 0.3 wt%. A volatile solvent, 2-chloropropane (Sigma-Aldrich Chem. Co.), was used to dissolve PIB before PIB was mixed with PB solvent and the 2-chloropropane in the mixture was removed using a vacuum rotary evaporator heated at the temperature of 35 °C. We assume that PIB does not precipitate because PB is a good solvent of PIB. In the following, 0.3 wt% PIB in PB will be named mBF (see Table I for other fluids).

B. Extension-induced mixer

To disperse CNT clumps as uniformly as possible, we devised a new system as shown in Fig. 2 and named "Extension-induced mixer." The basic idea of the design comes from the industrial spinning of cotton fiber from a wad of cotton. In drawing cotton fibers, cotton balls are stretched mechanically. Then cotton fibers are first aligned and then unraveled overcoming frictional forces due to entanglements of fibers. Here we use a very viscous fluid in stretching CNT clumps (since we cannot hold the micron sized CNT clumps using a solid holder) and we call this process "hydrodynamic dragging." A single pass of the stretching process of CNT by hydrodynamic dragging is not effective enough

TABLE I. Composition of suspensions.

Sample	Matrix	Concentration of carbon nantotube (wt%)	(vol%)
mBF	0.3 wt%PIB/PB	0	0
mBF01	0.3 wt%PIB/PB	0.1 wt% CNT/mBF	0.075
mBF03	0.3 wt%PIB/PB	0.3 wt% CNT/mBF	0.225
mBF05	0.3 wt%PIB/PB	0.5 wt% CNT/mBF	0.375
mBF10	0.3 wt%PIB/PB	1.0 wt% CNT/mBF	0.75
mBF15	0.3 wt%PIB/PB	1.5 wt% CNT/mBF	1.125
mBF20	0.3 wt%PIB/PB	2.0 wt% CNT/mBF	1.5

to unravel individual tubes. Therefore the stretching process has to be repeated to separate tubes from clumps effectively. The extension induced mixer was designed following this idea. An amount of viscoelastic fluid is continuously and periodically subjected to an extension-dominant flow between two parallel cylindrical bars connected to two counter rotating axes. During one cycle, the stretched band of fluid is folded at the center. The folding of the fluid band can make the mixer overcome the physical limitation of fluid-filament breakup that is frequently faced during extensive stretching of filaments.

The whole system of the extension-induced mixer consists of the extension (flow) part, the measuring part, and the power-transfer part. Figure 2(a) is the top view of the extension part connected to two counter-rotating gears of the power-transfer part. In the power-transfer part, there are three gears which make two axes (α_1 or α_2) rotating in the

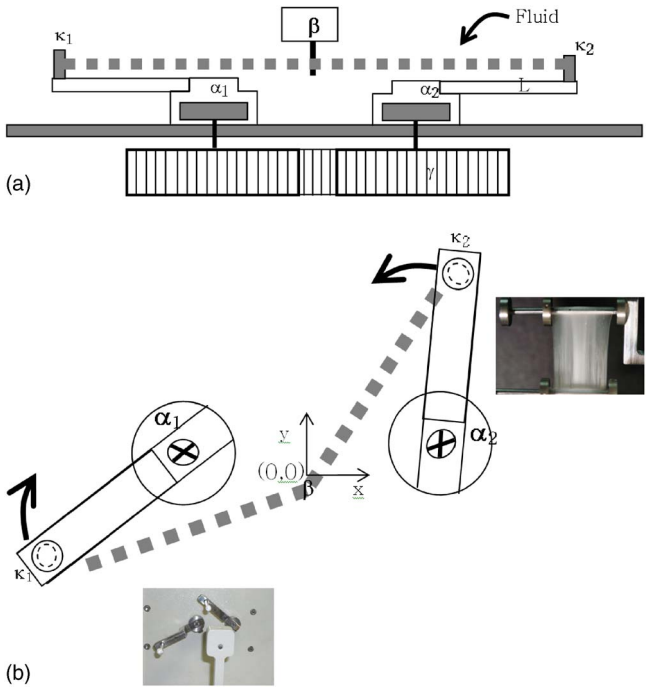

FIG. 2. Diagram of extension-induced mixer: (a) top view, (b) front view of extension-induced mixer. Two axes are rotating in opposite senses to extend and fold a viscoelastic liquid band continuously.

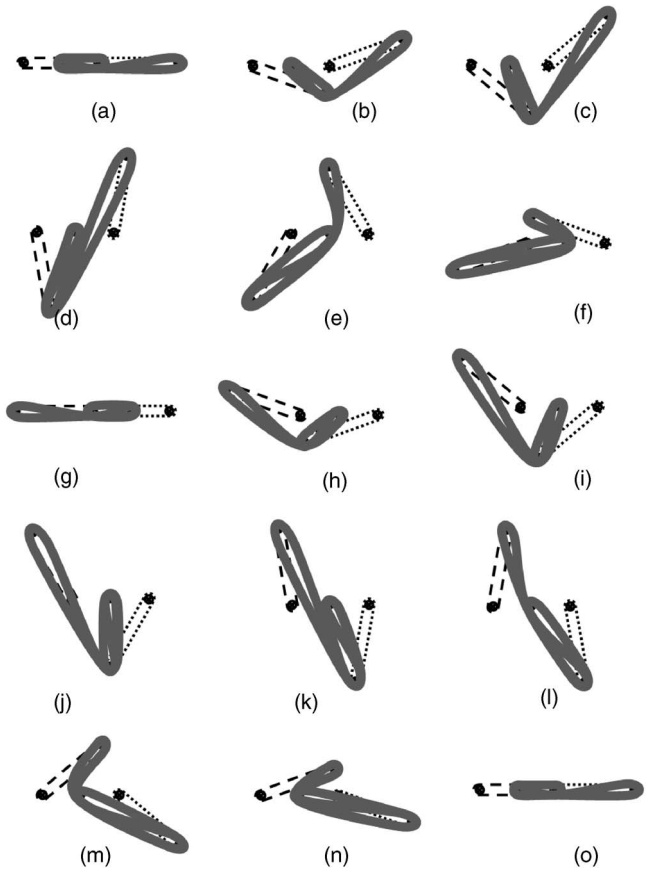

FIG. 3. Sequence of the extension-induced mixing mechanism for one cycle.

opposite sense. Between those two parts of the extension and the power transfer, a torque meter (Model 01424-310 with a signal amplifier, Sensor Developments Inc.) is installed to measure the torque needed to rotate the axis (not shown here) and hence to monitor the dispersion status. The extension part consists of two counter-rotating bars (κ_1, κ_2, left and right) and a stationary bar fixed to the stand (β). The three bars are parallel to each other and to the axis of the motor. Each rotating bar (κ_1 or κ_2) is fixed to a rotating arm (the arm length=L) that is perpendicularly extended from the axis (α) connected to the gear. The stationary bar (β) is placed at the center of the axes of the two rotating bars as shown in Fig. 2(b). The length of the rotating arm is 5 cm (But this can be varied depending on the elasticity of the fluid.) and it is the same as the distance ($2d$) between α_1 and α_2 which is variable depending on the fluid ($d<L$). The length of each bar is 5 cm which is also variable depending on the amount of fluid loaded. Figure 2(b) presents the diagram and photograph of the front view of the extension part. Between two bars (κ_1, κ_2), a proper amount of fluid (5.5–6.5 g) is loaded as depicted by a dotted line in Fig. 2(b) and then it is stretched repetitively by the counter-rotation of the two axes. To understand the rotation of two rotating bars and the deformation of fluid in the extension induced mixer, Fig. 3 presents the stepwise movement of two bars during one cycle and the stretching and bending of fluid band between them. In Fig. 3(a), β, κ_1 and κ_2 (from left to right) are collinear and both κ_1 and κ_2 are located at the positive x axis. As the κ_1 rotates clockwise

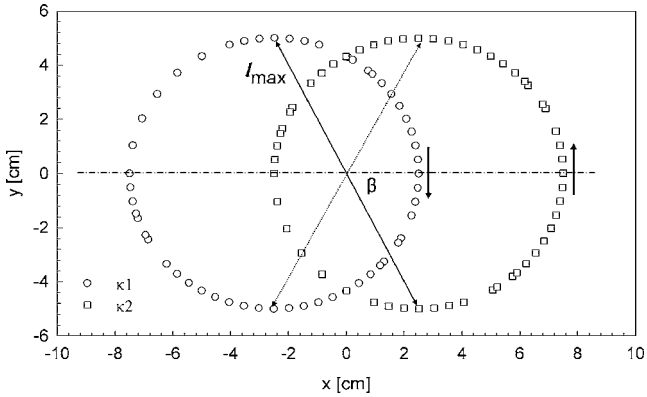

FIG. 4. Tracing of rotating bars.

and κ_2 rotates counterclockwise, the band between β and κ_2 begins to be bent and the fluid element between κ_1 and κ_2 has the minimum length, $l_{\min}$ which is the same as the length of the arm A. The fluid element continues to be stretched until κ_1, β and κ_2 become collinear again after rotation of $\pi/2$ [Fig. 3(d)] while the fluid element held by β and κ_2 is less stretched than the fluid band between κ_1 and κ_2. At this configuration the stretched fluid element between κ_1 and κ_2 has the maximum length $l_{\max}$ which is given as follows:

$$l_{\max} = 2\sqrt{d^2 + L^2}, \tag{1}$$

where d is the half distance between two rotating axis and L is the length of rotating arm (if $d=L/2$, $l_{\max}=\sqrt{5}L$). As the rotation continues the stretched element begins to be bent by β [Fig. 3(e)] and the fluid element held between β and κ_1 is contracted until κ_1, κ_2 and β are collinear in this order after the rotation of another $\pi/2$ [Fig. 3(g)] while the fluid element between β and κ_2 is stretched from $l_{\max}/2$ to $L+d$. Both the stretched and contracted part have the length of $l_{\max}/2$. During this period, the fluid element held between β and κ_2 is contracted from $l_{\max}/2$ to L-d. As the motion continues we have the same pattern of deformations between 0 and π (Figs. 3(a)–3(g)) during π and 2π [Fig. 3(h)–3(o)] while the fluid element that is mostly stretched being exchanged from the element from β and κ_2 to κ_1 and β. Therefore, the whole cycle repeats while being stretched and mixed as the motion continues. The counter-rotations of two rotating axes (α_1, α_2) are described according to the following relationships:

$$x_1 = -d - L\cos(2\pi\varpi t/60), \quad y_1 = L\sin(2\pi\varpi t/60),$$

$$x_2 = d - L\cos(2\pi\varpi t/60), \quad y_2 = -L\sin(2\pi\varpi t/60), \tag{2}$$

where ϖ (the number of rotation/min) is rotor speed and the origin of the coordinates is fixed at the position of the stationary bar (β).

When two axes (α_1, α_2) are rotating with the speed (ϖ) of 10 rpm, Fig. 4 shows the tracing of $\kappa_1(x_1, y_1)$, $\kappa_2(x_2, y_2)$ for one cycle. During one cycle, the fluid between two rotating bars (κ_1, κ_2) is stretched up to the maximum length ($l_{\max}$) twice when two axes (α_1, α_2) are rotated by $\pi/2$ [Figs. 3(d) and 3(k)] from the collinear position of three bars [$y=0$; see Figs. 3(a) and 3(g)]. For stretching of the fluid band, the apparent extensional deformation can be defined without considering the folding. If the initial length of a fluid

band is l_o and the fluid band is stretched to l during the time span of Δt, the rate of stain becomes $\Delta(l/l_o)/\Delta t$. Then, if l increases as much as $2l_{\max}$ for every cycle the apparent deformation rate is as follows:

$$\dot{\varepsilon}_{app} = \frac{2\ell_{\max}}{\ell_o}\frac{\varpi}{60}, \tag{3}$$

where $\dot{\varepsilon}_{app}[1/\mathrm{s}]$ is the apparent strain rate of fluid and it is assumed that l_o is the same as L that is the minimum length of the fluid element. Then $\dot{\varepsilon}_{app}$ is proportional to ϖ ($\dot{\varepsilon}_{app} \approx 0.075\varpi$). Given $\dot{\varepsilon}_{app}$, Weissenberg number for the extensional flow in the mixer is defined as follows:

$$We = \lambda_1 \dot{\varepsilon}_{app} \approx 0.075\lambda_1\varpi, \tag{4}$$

where λ_1 is the relaxation time of fluid. In the case of Boger fluid, it can be predicted from the Oldroyd-B model and λ_1 for mBF is found to be 5.68 s (calculated from Fig. 8). For $\dot{\varepsilon}_{app}$ between 10 and 30 rpm *We* varied from 4.3 to 12.8.

To monitor the status of extensional flow in this equipment, a torque sensor is installed between the gear box and the rotating axis. When a fluid element loaded between two rotating bars (κ_1, κ_2) is deformed by the rotation of the two axes (α_1, α_2), the torque sensor measures the torque value needed to rotate the axis (α_1) at a given rotational speed. The variation of torque with time will reflect the change of stress at least indirectly (Because the cross section of the fluid band along the stretching direction changes as the fluid band deforms, we can measure only the force). Then the monitoring of torque in real time gives an important indication in the fiber suspension since its orientation, distribution, and fiber-fiber interaction are reflected on the stress of suspension.

Figure 5(a) shows the torque before a fluid is loaded. We note that the torque changes sinusoidally even without a sample due to the weight of the arm and the bar themselves. The torque has a positive value due to the same direction of rotating axis (α_1) with the gravity when the arm κ_1 is moving between Fig. 3(e) and Fig. 3(k). It has a negative value when it is between Fig. 3(l) and the next cycle of Fig. 3(d). Figure 5(b) shows the torque measured between 150 and 160 s after mBF is subjected to flow. With a fluid, the torque shows two peaks during one full rotation of 360°. The first peak of them is the torque when the rotating bar begins to stretch the fluid element from the folded state and the second peak is the torque when a fluid is stretched to the maximum stretching position. The first peak is larger than the second one because the bar begins to stretch the folded fluid [Case Fig. 3(e)]. The second one is the torque needed only to stretch a fluid band without being folded [Case Fig. 3(b)]. The measured torque will be a function of the mass of a fluid and its angular velocity. To exclude the effect of the mass on torque, the measured torque was normalized by dividing torque values by the total mass loaded on the mixer.

C. Preparation of CNT suspensions

To disperse the CNT clumps in fluid, CNT powders were added to the fluid band just after a fluid (mBF) was loaded onto the mixer and a stable band of the fluid was formed between two bars of the mixer. The formulations of CNT suspensions prepared in this study are listed in Table I. The naming convention of the sample is such that, for example, mBF01 is the mBF suspension containing 0.1 wt% of CNT powder.

CNTs were dispersed at four different angular velocities, 10, 15, 20, and 30 rpm, corresponding to $\dot{\varepsilon}_{app}$ of 0.75, 1.13, 1.5, and 2.26 1/s, respectively. We did not modify the surface of CNT by an acid-treatment or ultrasonication method to improve the dispersion

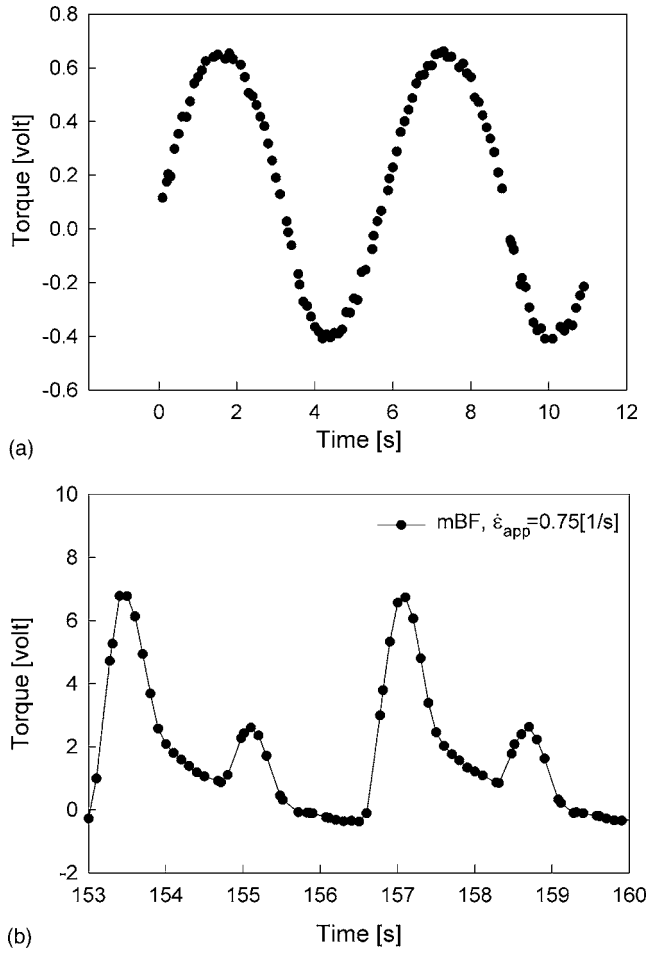

FIG. 5. Torque measurement (a) of rotating bar with time and (b) its variation after being loaded with mBF in extension-induced mixer. In (a), even without a loaded sample torque shows a periodic variation due to the weight of the arm and bar. With a loaded sample, the torque shows a double periodic variation. The larger peak corresponds to the extension of a folded band while the smaller peak corresponds to the extension of a single band.

characteristics of CNT. For the comparison of the dispersion of CNT prepared by the extension-induced mixer, mechanically stirred and hand-mixed CNT dispersions were also prepared. For mechanically stirred mBF03, 0.3 wt% CNT was added to mBF and then the suspension was mechanically stirred with a screw stirrer (RW20DZM.nP4, LABORTECHNIK) at 10 rpm for 2 h to avoid breakage or damage of CNT. The hand-mixed mBF03 dispersion was prepared by hand mixing using a spatula.

D. Rheological measurements and morphology observations

The rheological properties of fluids and CNT suspensions were measured using a stress-controlled rheometer (AR2000 of TA instruments) with a parallel plate fixture (diameter 35 mm). The gap distance between the two plates was set at 0.9–1.2 mm to prevent wall effects on measurement [Blakeney, 1966; Attanasio *et al.* (1972)]. For steady shear viscosity, steady stress sweep tests were conducted over the stress range

from 0.1 to 100 Pa. Small amplitude oscillatory shear tests were conducted over the frequency (ω) range from 0.1 to 200 rad/s to measure the viscoelastic properties. The bulk density of CNT ($>1000-1300\ \mathrm{kg/m^3}$) is larger than the suspending fluid ($890\ \mathrm{kg/m^3}$) and this difference between CNT and suspending medium densities possibly causes the sedimentation of CNT clumps. To minimize the effect of sedimentation, the rheological measurements were carried just after the mixing using the extension-induced mixer. All experiments were carried out at 298 K.

The morphology of CNT was observed using a scanning electron microscope (JSM 840A, JEOL) [See Fig. 1(a)]. The suspension morphology was observed using an optical microscope (OM; BX51, Olympus) equipped with the Cambridge Shearing System (Linkam CSS-450) and the cryo-transmission electron microscopy (Cryo-TEM). Using OM, the change of suspension morphology under shear flow could be observed at a low magnification level. The microscopic structure of the CNT-dispersed suspension by the extension-induced mixer was further investigated using Cryo-TEM. The suspension was imaged at $-170\ ^\circ\mathrm{C}$ using JEOL 1200EXII TEM equipped with a Gatan 626 cold stage.

III. RESULTS AND DISCUSSION

A. Dispersion of CNT by shear flow

CNT powders are difficult to disperse by itself due to the tendency of CNT to aggregate by van der Waals force between them. It is more difficult to disperse CNT in a viscous liquid because the diffusivity of CNT powder is decreased with the viscosity (η_s) of suspending medium. In this experiment it is observed that CNTs have a strong tendency to clump into several hundreds micron-sized agglomerates under shear flow. Figure 6(a) is a picture of mBF hand mixed with 0.5 wt% CNT and Fig. 6(b) for the mBF05 mechanically mixed for 2 h at a low speed of 10 rpm. Even under hand mixing, CNTs rather clump into aggregates. When mBF05 is mechanically stirred, the CNT clumps of hundred microns are still observed even though the huge CNT aggregates that are frequently observed for hand-mixed samples are not observed any more. When the mechanically stirred mBF05 in Fig. 6(b) is subjected to the shear flow of 1 1/s for 1 h, the aggregation of CNT clumps progresses further. As the concentration of CNT in the fluid increases, CNT clumps aggregate to a larger one as shown in Fig. 6(c). Under shear flow, CNT clumps are rotated and large CNT clumps can approach each other. Then they stick together eventually as they contact each other. Therefore we may argue that simple shear flows are not effective enough to disperse CNT clumps into individual carbon nanotubes and rather they even induce aggregation. Even though highly viscoelastic fluids such as a Boger fluid are used as a suspending medium to induce homogeneous distribution against the alignment of particles under shear flow [Scirocco *et al.* (2005)], the aggregation of CNT clumps in a high viscoelastic fluid is frequently observed due to strong van der Waals forces originated from the large contact area of CNT. Being different from shear flow, the extensional flow seems to be more effective to disperse CNT clumps. For example, when mBF05 samples are subjected to the extensional flow for 1 h in the extension-induced mixer we get enhanced dispersion of CNT as shown in Fig. 6(d). In the following section, the dispersion of CNT under extensional flow is further investigated and the rheological behavior of CNT suspension is studied.

B. Dispersion of CNT by extension-induced mixer

The disentanglement of individual tubes from CNT clumps was attempted by inducing the hydrodynamic dragging between CNT and the highly viscous suspending medium under shear flow. But, as shown in the previous section, the shear flow has been found to

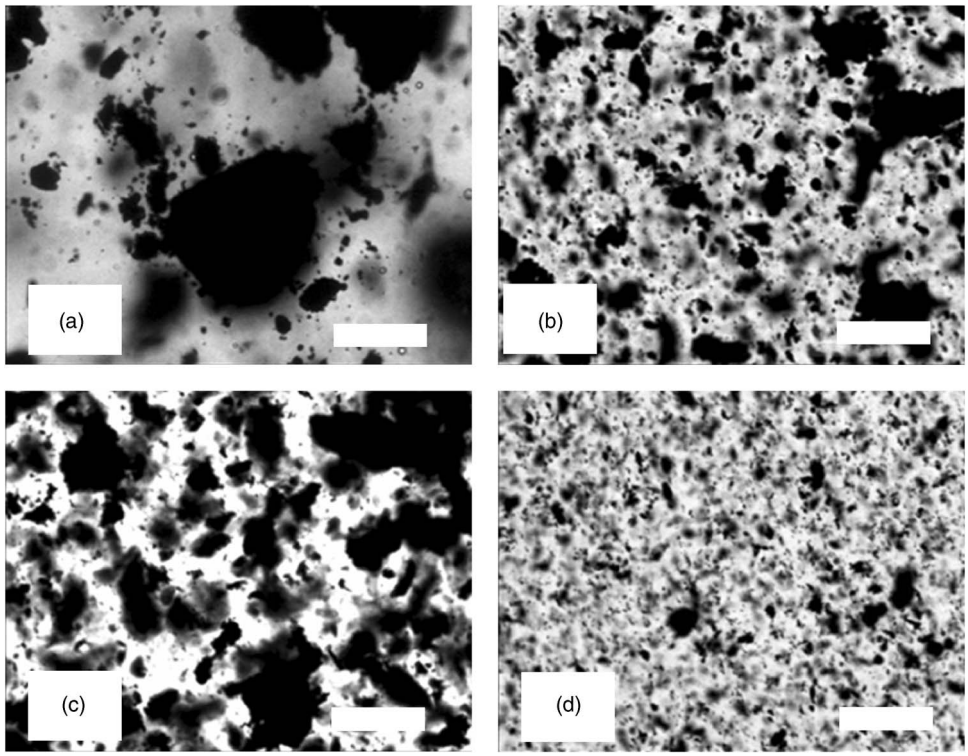

FIG. 6. Optical microscopic pictures of (a) hand-mixed mBF05, (b) mechanically mixed mBF05, and mBF05 (c) under shear flow and (d) under extensional flow. Scale bar is 100 μm.

be neither effective nor strong enough to disperse individual tubes from CNT clumps. Therefore, we investigated the possibility of applying extensional flows to unravel tubes from the clump. When the concentration of CNT is very dilute, it will be possible to disperse an individual CNT from CNT clumps by pulling the both ends if the hydrodynamic force transferred from suspending medium is dominantly larger than the van der Waals force between CNTs. Using the extension-induced mixer, we can maintain the process of hydrodynamic dragging for a long period to unravel individual tubes from clumps.

First of all, mBF as the matrix was subjected to the extensional flow for 3 h at $\dot{\varepsilon}_{app}$ of 1.13 1/s without adding CNTs. Next we investigated the mixing effect by adding CNTs. In Fig. 7, the viscosity of mBF is compared before and after the imposition of the extensional flow together with the change in viscosities by the addition of 0.5 wt% CNT before and after the extensional flow. The mBF shows slightly shear-thinning behavior. When mBF is stretched for 3 h in the extension-induced mixer, the viscosity of mBF is reduced from 48 Pa s (at 0.1 Pa) to 34 Pa s (at 0.1 Pa) by the degradation of long PIB chains. In extensional flows polymer chains of high M_w can be broken at high *We*, say larger than 1 [Keller and Odell (1985); Larson (1999)]. Since the *We* for this study is between 4.3 and 12.8, long PIB chains should be broken due to the extensional flow. The reduction of M_w of polymer chain is well reflected on the dynamic rheological property of mBF in Fig. 8. The storage moduli of both mBFs are proportional to ω^2 but the terminal zone shifts to higher frequency after the imposition of extensional flow for a long time. In the terminal zone, the rheological behavior is dominated by the longest

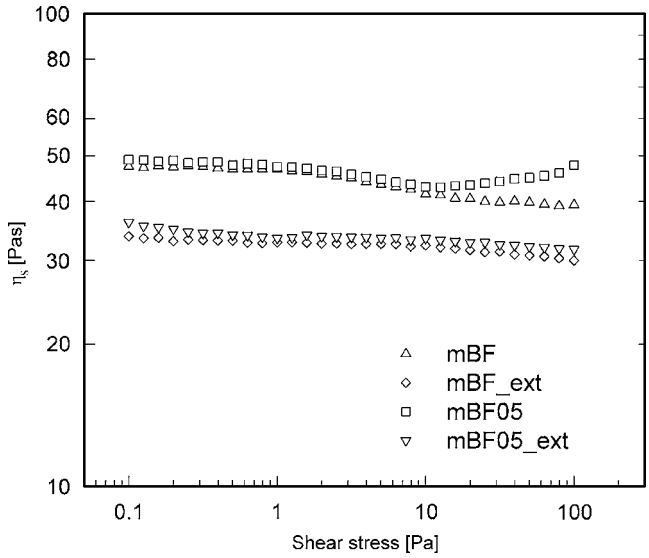

FIG. 7. Comparison of viscosity of mBF, extended mBF for 3 h, hand mixed of 0.5 wt% CNT with mBF or extended mBF.

relaxation time ($\lambda \propto M_w^2$, for very dilute solution of Rouse chains). If the longest relaxation time (λ_1) is calculated from the Oldroyd-B model, λ_1 of mBF is reduced from 5.68 to 3.98 s after the imposition of extensional flow for 3 h. Also, gel permeation chromatography (GPC) test of mBF1 shows that the number average molecular weight of PIB chain (M_n) is reduced to 1.04 M from 3.1 M by stretching of mBF1 for 3 h (not shown here). The hand mixing of mBF05 does not result in a substantial increase in the viscosity of suspension by the addition of 0.5 wt% CNT. As seen in Fig. 7, the viscosity of mBF05

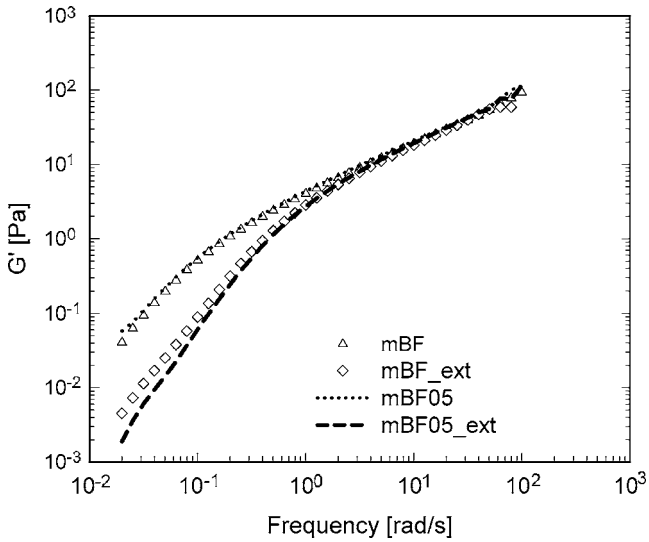

FIG. 8. Comparison of storage moduli of mBF, extended mBF for 3 h, hand-mixed mBF with 0.5 wt% CNT and extended mBF. Due to degradation, terminal values are lowered for extended samples.

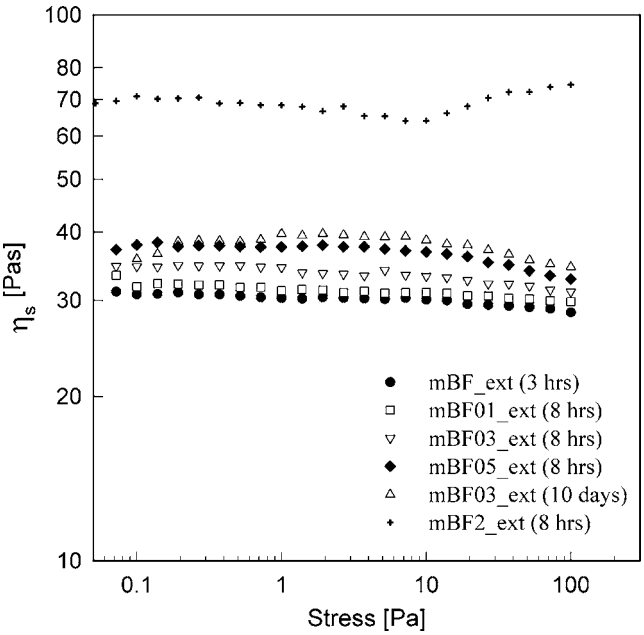

FIG. 9. Viscosity of mBF suspensions with CNTs. As mixing time increases, viscosity increases. The increase is more conspicuous with more CNTs.

suspension is mostly the same as the viscosity of mBF itself though mBF degraded by the extensional flow for a long time shows a slight increase in viscosity by the addition of 0.5 wt% CNT. From Figs. 7 and 8, it can be argued that the poorly dispersed CNT clumps do not increase the viscosity of suspension.

In the next we have described the result when CNT was added to mBF and stretched in the extension-induced mixer for several hours. First of all, as the stretching process went on, we observed that the size of CNT clumps became smaller and smaller. Figure 9 shows that the viscosity of CNT suspension increases with the concentration of CNT. The Einstein theory on the viscosity of dilute suspension of spheres without the Brownian effect and particle-particle interaction predicts that the viscosity increase will be only 0.86% if 0.5 wt% of CNT (0.34 vol%) is added to a Newtonian solvent assuming that the CNT clumps have essentially the spherical shape. Beyond this expectation, the viscosity is increased more than 20% by the addition of 0.5 wt% CNT ($\eta_{\text{mBF\_ext}}$=31 Pa s and $\eta_{\text{mBF05\_ext}}$=37.6 Pa s at 1 Pa). This is the manifestation of the fact that the individual CNT of high aspect ratio is unraveled from the CNT clumps and the contribution of those unraveled CNTs to the effective hydrodynamic volume is increased. According to the theory of Batchelor (1971), when the average distance between individual CNTs of high aspect ratio is less than one half length of the nanotube the hydrodynamic interaction between nanotubes will play an important role in the increase of their rheological properties. In the case of mBF03 suspension, when the extensional flow is imposed continuously for ten days, the viscosity is increased more than 30% through further unraveling of individual CNTs from its clumps ($\eta_{\text{mBF\_ext}}$=31 Pa s and $\eta_{\text{mBF03\_ext}}$=39.7 Pa s at 1 Pa) despite the fact that polymer chains or individual nanotubes should be broken up severely by further stretching. In Fig. 10, it can be seen that CNT clumps of 10 μm or larger are not observed anymore when examined using OM (Magnification of 100). Since microscopic techniques cannot be an adequate method of characterizing the mixing status due

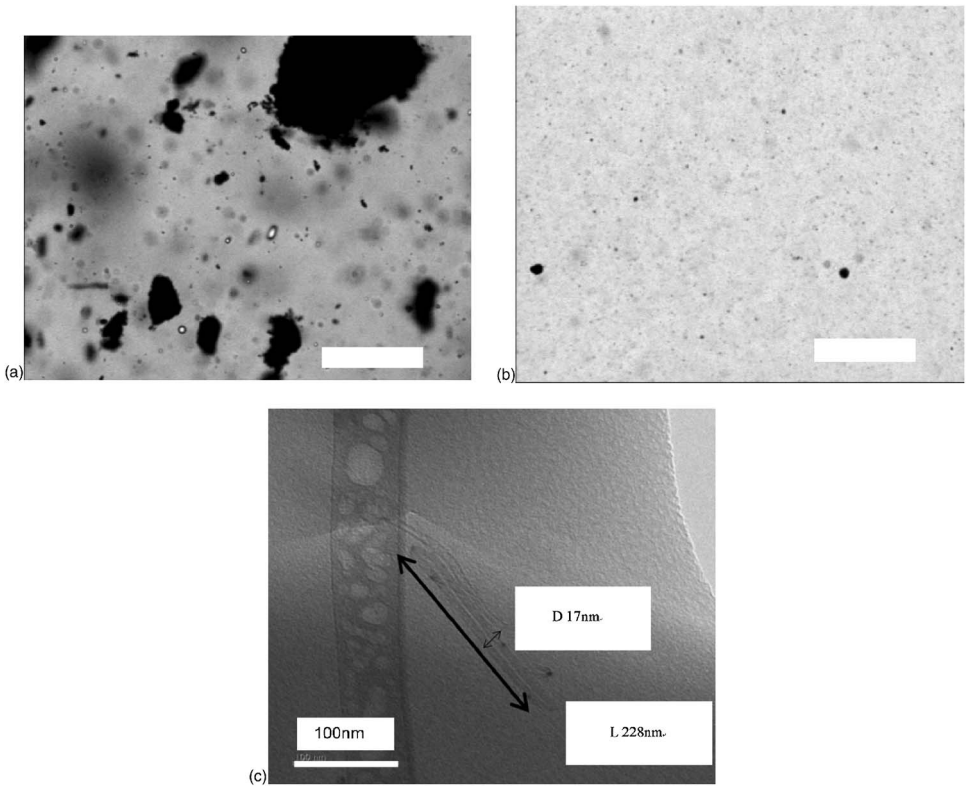

FIG. 10. OM pictures of (a) hand-mixed mBF03, (b) mBF03 under extensional flow for ten days, and (c) its Cryo-TEM picture. Scale bar is 100 μm.

to the short length scales of CNT [Huang *et al.* (2006)], we cannot claim that the dispersion is well dispersed from the microscopic data. However, we may notice that the dispersion is much more improved by using the extensional mixer. Also, even though we cannot argue that all the CNTs are unraveled, cryo-TEM shows that at least some of the CNT clumps are disentangled into individual tubes as shown in Fig. 10(c). In the extension mixer the average stress exerted to nanotubes can be estimated from the torque data. At the initial stage of mixing, it has an order of 10^5 J/m^3. This value is larger than the van der Waals energy of 10^4 J/m^3 holding the CNT aggregates together estimated by Huang *et al.* (2006). Therefore, it was possible to disintegrate the aggregate. However, it drops to 10^4 J/m^3 at the final stage of mixing due to the degradation of polymer. This minimum value is comparable to the van der Waals energy of CNT. But in this state many of the CNT clumps are already disentangled. Also, the extensional flow is much more efficient compared to shear flow because in shear flow much of the energy is dissipated rather than used for disentanglement.

As the CNT content increases to 2 wt%, it was difficult to maintain the extensional flow for a long time since the addition of 2 wt% CNT made mBF less elastic. However, the viscosity increased much larger. This increased viscosity is mostly attributed to the interaction between CNTs induced by the mechanical and hydrodynamic contact and the increased hydrodynamic interaction between CNT clumps.

To further investigate the rheological properties of CNT dispersion, mBF05 and mBF15 were subjected to the extensional flow of different extensional rates. Figure 11

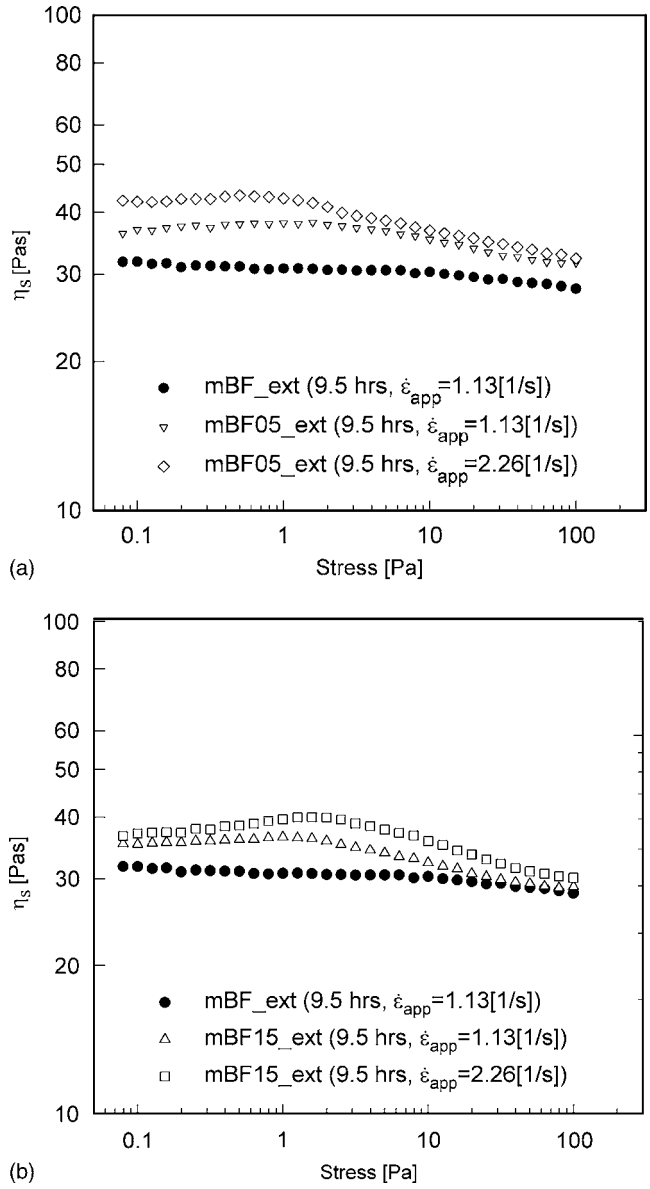

FIG. 11. Comparison of viscosity of mBF05, mBF15 extended at different rates for 9.5 h. Higher extensional rate gives larger change in viscosity.

compares their viscosities after imposing the extensional flow for 9.5 h. Both of suspensions show that their viscosity increases as $\dot{\varepsilon}_{app}$ increases by the application of the larger strain rate. Moreover, mBF15 shows larger increase in its viscosity. We believe that this is due to the interaction among the CNT clumps with reduced sizes. When $\dot{\varepsilon}_{app}$ is 2.26 1/s, the maximum torque described in Fig. 5 is presented with extension time in Fig. 12. The behavior of mBF with extension time dominantly leads the variation of torque and the maximum torque of three fluids consistently decreases as the extension time goes on. The maximum torque appears to be decreased by the severe degradation of base polymer solution under the extensional flow.

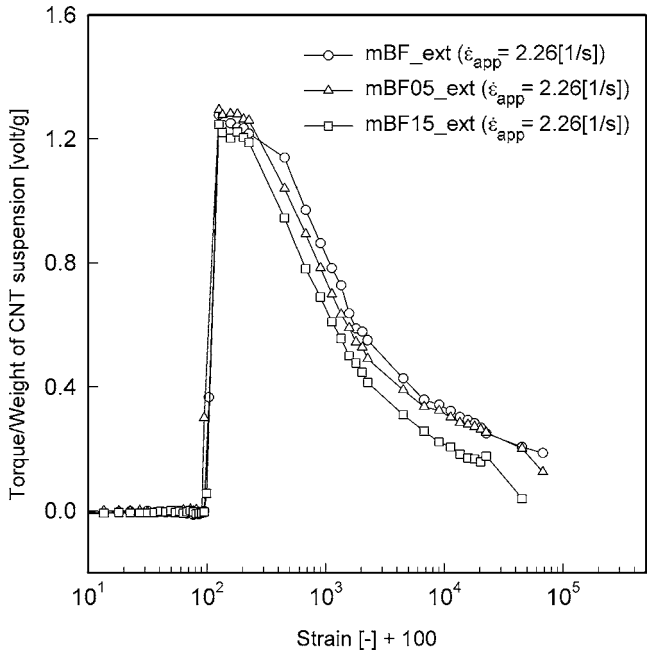

FIG. 12. The maximum torque of mBF, mBF05, mBF15 under extensional flow at the extensional rate of 2.26 1/s for 9.5 h. Due to degradation, the torque decreases continuously with time. Strain is obtained by multiplying mixing time. Here we added 100 to strain value to avoid the problem at zero strain in logarithmic plot.

The time traces of torque variation of CNT suspension are plotted for differing CNT contents at $\dot{\varepsilon}_{app}$ of 2.26 1/s in Fig. 13. Figure 13(a) is the torque variation between 150 and 155 s just after the imposition of the extensional flow and Fig. 13(b) is the torque variation of mBF05 after extension for 9.5 h and after 6.5 h for mBF15. The maximum torque is normalized with the value at the extension time of 150 s. At the beginning stage of 150 s, it is difficult to expect a large effect of the addition of a small amount of CNT. Also, unraveling of individual tubes cannot be progressed. Then, the torques for mBF and CNT suspension are nearly identical for the same masses of mBF or mBF05 loaded on the extension-induced mixer. At this time the torque value at an extension point (the minor peak) is 40% of the maximum torque (the major peak). However, after being subjected to the extensional flow for a long time, the maximum torque is reduced to 20% of the torque value at 150 s due to degradation of polymers. However, at the extension point, the ratio of the extension peak against the maximum torque is increased from 40% to 60–70% reflecting the dispersion of CNTs. In the case of $\dot{\varepsilon}_{app}$=0.75 1/s, the ratio of the extension peak and the maximum torque at early stage of the total extension is listed in Table II. After extension for 7500 s, the maximum torque of mBF05 or mBF15 has reduced to about 20% of the initial maximum value. However, the ratio of extension peak and the maximum torque value is increased more than 100% and also it is more increased for highly loaded suspension (mBF15). In other words, although the absolute value of the extension peak is reduced by the degradation of polymer chains and possibly some nanotubes too, the ratio of the extension peak and the maximum torque is increased by the contribution of unraveled carbon nanotubes. The polymer contribution to extensional viscosity ($\eta_{p,\infty}$) at high extension rate is proportional to the extendibility parameter of chain (B). Parameter B is three times the square of the ratio of the polymer's fully

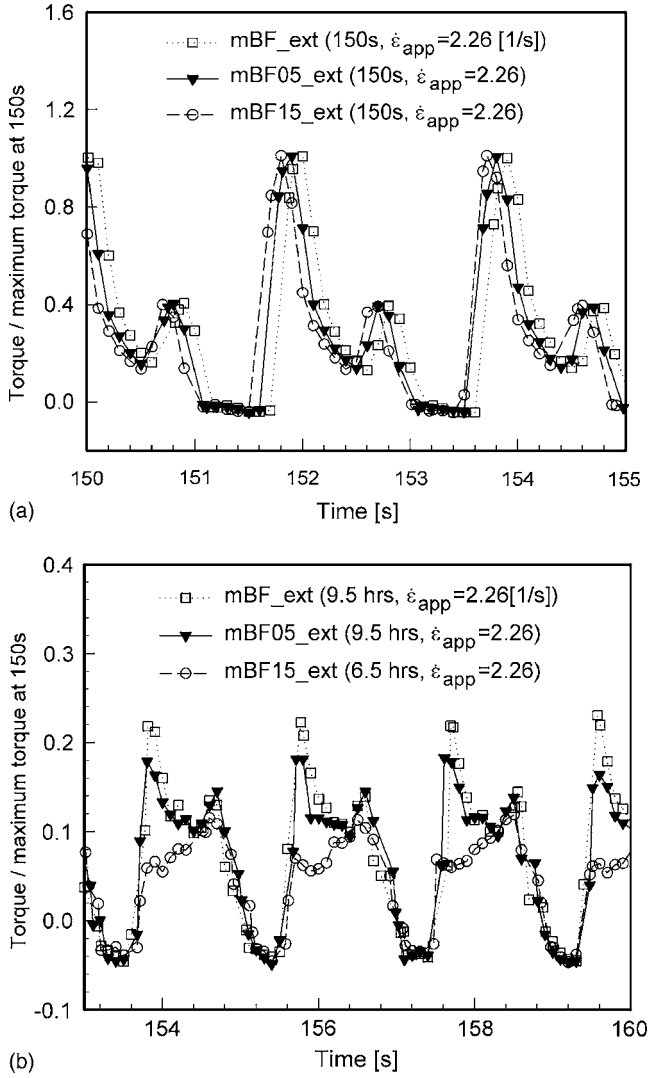

FIG. 13. Comparison of torque for a rotation of mBF05, mBF15 (a) after 150 s and (b) 9.5 h under extensional flow at the extensional rate of 2.26 1/s.

extended length (L_e) to its root-mean-square end-to-end distance ($\langle R^2\rangle_o$) and it is proportional to M_w of polymer ($B=3L_e^2/\langle R^2\rangle_o \propto M_w$, $L_e \propto 1.54$ n, $\langle R^2\rangle_o \propto 1.54$ nC$_\infty$, $n=M_{w,\mathrm{PIB}}/28$, $C_\infty=6.8$, $M_w=3.1$ M for PIB) [Larson (1999)]. As stated early in this section, the M_w of polymer is degraded from 3.1 to 1.04 M by stretching. The change in the maximum torques appears to reflect the degradation of polymer reasonably well. The ratio of the extension peak and the maximum torque is found to be increased from 37 to 40% to 60–140% by the alignment of individual carbon nanotubes. If CNTs are aligned, the shear viscosity will be almost the same as the viscosity of the fluid itself because the rotation of the tube is restricted. But the extensional viscosity should increase dramatically. For example, when the volume % is 0.35 ($\phi=0.0035$) and the $L/d=p=1000$ (here it is very close to our CNTs), the extensional viscosity will be about 700 times larger than the shear viscosity if we apply the theory of Batchelor (1971):

TABLE II. Maximum torque and its ratio with extension peak of mBF05 and mBF15.

Suspensions		Extension time [s]	Maximum torque (torque/weight of suspension) [volt/g]	Extension peak/maximum torque [–]
mBF05	$\dot{\varepsilon}_{app}=0.75$	0	1.32	0.37
		300	0.92	0.40
		7500	0.22	0.79
mBF15	$\dot{\varepsilon}_{app}=0.75$	0	1.35	0.4
		300	0.83	0.43
		7500	0.18	0.97

$$\frac{\eta_e}{3\eta_s} = 1 + \frac{4\phi p^2}{9\ln(\pi/\phi)}. \tag{5}$$

However, the increase in viscosity is far less than the predicted value. We may surmise that the unraveling is not complete and only a fraction of individual tubes were unraveled. Also, the extensional deformation is less than 2.25 for each half cycle and the time of the imposition of the extension is too short to reach the steady alignment of CNTs. Therefore, we cannot have such a large value of extensional viscosity. If we use a long arm to impose a stronger extensional flow, however, the degradation of polymer will be even more significant. Also, the polymer chains will be degraded more severely in the CNT mixture than in pure polymer solutions due to the increased stress level. When the CNT content is increased from 0.5 to 1.5 wt%, it was found to be difficult to continue the flow up to 9.5 h by the reduced elasticity of mBF with the addition of large amount of CNT and physically the fluid band was broken.

As observed in the above, the extension-induced mixer can subject CNT suspension to an extensional flow for a long time and it is demonstrated that the continuous application of the hydrodynamic dragging to CNT clumps induces the pullout of individual tubes from entangled clumps. Because the extension-induced mixer realizes a continuous extensional flow, the usage of this devise can be widened by applying to mixing of two different fluids even though two fluids have a large difference in viscosity. For example, 30 wt% polydimethylsiloxane (PDMS, KF-96H-10,000cs, Shin-Etsu Chem. Co., Ltd.) was mixed with Boger fluid (η=25 Pa s) in the extension-induced mixer for 1 h and the averaging droplet size of the dispersed phase was lowered below 3 μm.

IV. CONCLUSIONS

In this study, we have proposed a new mixing and dispersing system named an extension-induced mixer to disperse carbon nanotube clumps into individual tubes by imposing hydrodynamic force continuously and periodically. The new system has been found to be effective in unraveling individual tubes from the CNT clumps by the action of hydrodynamic forces. Rheological measurements and microscopic observations confirm the unraveling of tubes. However, due to severe degradation of polymeric base fluids, it was not possible to continue to impose the extensional flow indefinitely and hence it was not possible to unravel most of the individual tubes from the clumps. If one can find a more effective viscoelastic base fluid, the unraveling of tubes will be more close to completion. Even though unraveling is not complete, the new system is found to be very effective in reducing the clump size. This is a very noticeable point in that shear

flows even formed larger, weakly bound agglomerates with diameters up to millimeters. The newly suggested mixing technique can be used effectively for mixing two different kinds of polymer melts with a large difference in viscosity.

ACKNOWLEDGMENT

The authors wish to acknowledge the Korean Science and Engineering Foundation (KOSEF) for the financial support through the Applied Rheology Center (Project Number: R0602211), an official engineering research center (ERC) in Korea.

References

Attanasio, A., U. Bernini, P. Galloppo, and G. Segre, "Significance of viscosity measurements in macroscopic suspensions of elongated particles," Trans. Soc. Rheol. **16**, 147–154 (1972).

Bandyopadhyaya, R., E. Nativ-Roth, O. Regev, and R. Yerushalmi-Rozen, "Stabilization of individual carbon nanotubes in aqueous solution," Nano Lett. **2**, 25–28 (2002).

Bar-Chaput, S., and C. Carrot, "Rheology as a tool for the analysis of the dispersion of carbon filler in polymers," Rheol. Acta **45**, 339–347 (2006).

Batchelor, G. K., "The stress generated in a non-dilute suspension of elongated particles by pure straining motion," J. Fluid Mech. **46**, 813–829 (1971).

Blakeney, W. R., "The viscosity of suspensions of straight rigid rods," J. Colloid Interface Sci. **22**, 324–330 (1966).

Dwyer, C., M. Guthold, M. Falvo, S. Washburn, R. Superfine, and D. Erie, "DNA-functionalized single-walled carbon nanotubes," Nanotechnology **13**, 601–604 (2002).

Harris, P. J. F., *Carbon Nanotubes and Related Structures: New Materials for the Twenty-First Century* (Cambridge University Press, Cambridge, 1999).

Huang, Y. Y., S. V. Ahir, and E. M. Terentjev, "Dispersion rheology of carbon nanotubes in a polymer matrix," Phys. Rev. B **73**, 125422 (2006).

Iijima, S., "Helical microtubules of graphitic carbon," Nature (London) **354**, 56–58 (1991).

Keller, A., and J. A. Odell, "The extensibility of macromolecules in solution: A new focus for macromolecular science," Colloid Polym. Sci. **263**, 181–201 (1985).

Larson, R. G., *The Structure and Rheology of Complex Fluids* (Oxford University Press, New York, 1999).

Li, D., H. Wang, J. Zhu, X. Wang, L. Lu, and X. Yang, "Dispersion of carbon nanotubes in aqueous solutions containing PDMA," J. Mater. Sci. Lett. **22**, 253–255 (2003).

Magda, J. J., and R. G. Larson, "A transition occurring in ideal elastic liquids during shear flow," J. Non-Newtonian Fluid Mech. **30**, 1–19 (1998).

Matarredona, O., H. Rhoads, Z. Li, and J. H. Harwell, "Dispersion of single-walled carbon nanotubes in aqueous solutions of the anionic surfactant NaDDBS," J. Phys. Chem. B **107**, 13357–13367 (2003).

Sano, M., J. Okamura, and S. Shinkai, "Colloidal nature of single-walled carbon nanotubes in electrolyte solution: The Schulze-Hardy rule," Langmuir **17**, 7172–7173 (2001).

Scirocco, R., J. Vermant, and J. Mewis, "Shear thickening in filled Boger fluids," J. Rheol. **49**, 551–567 (2005).

Xu, J., S. Chatterjee, K. W. Koelling, Y. Wang, and S. E. Bechtel, "Shear and extensional Rheology of carbon nanofiber suspensions," Rheol. Acta **44**, 537–562 (2005).

Zhou, B., Y. Lin, H. Li, W. Huang, J. W. Connell, L. F. Allard, and Y. Sun, "Absorptivity of functionalized single-walled carbon nanotubes in solution," J. Phys. Chem. B **107**, 13588–13592 (2003).